The combined effect of side-coupled gain cavity and lossy cavity on the plasmonic response of metal-dielectric-metal surface plasmon polariton waveguide

2014 J. Phys.: Condens. Matter 26 255301

(http://iopscience.iop.org/0953-8984/26/25/255301)

IOP Publishing Journal of Physics: Condensed Matter
J. Phys.: Condens. Matter **26** (2014) 255301 (7pp) doi:10.1088/0953-8984/26/25/255301

The combined effect of side-coupled gain cavity and lossy cavity on the plasmonic response of metal-dielectric-metal surface plasmon polariton waveguide

Qiong-gan Zhu[1], Wei Tan[2] and Zhi-guo Wang[1,2]

[1] School of Physics Science and Engineering, Tongji University, Shanghai 200092, People's Republic of China
[2] Beijing Computational Science Research Center, Beijing, 100084, People's Republic of China

E-mail: zgwang@tongji.edu.cn

Received 5 January 2014, revised 14 April 2014
Accepted for publication 17 April 2014
Published 27 May 2014

Abstract

The combined effect of side-coupled gain cavity and lossy cavity on the plasmonic response of metal-dielectric-metal (MDM) surface plasmon polariton (SPP) waveguide is investigated theoretically using Green's function method. Our result suggests that the gain and loss parameters influence the amplitude and phase of the fields localized in the two cavities. For the case of balanced gain and loss, the fields of the two cavities are always of equi-amplitude but out of phase. A plasmon induced transparency (PIT)-like transmission peak can be achieved by the destructive interference of two fields with anti-phase. For the case of unbalanced gain and loss, some unexpected responses of structure are generated. When the gain is more than the loss, the system response is dissipative at around the resonant frequency of the two cavities, where the sum of reflectance and transmittance becomes less than one. This is because the lossy cavity, with a stronger localized field, makes the main contribution to the system response. When the gain is less than the loss, the reverse is true. It is found that the metal loss dissipates the system energy but facilitates the gain cavity to make a dominant effect on the system response. This mechanism may have a potential application for optical amplification and for a plasmonic waveguide switch.

Keywords: gain, loss, surface plasmons, integrated waveguide

(Some figures may appear in colour only in the online journal)

1. Introduction

Surface plasmon polaritons (SPPs) have been used to overcome the diffraction limit and manipulate light in the nanoscale domain, thus they are regarded as one of the most promising technologies for the minimization of integrated waveguides [1, 2]. However, a major obstacle for broader applications of SPPs is tied up with the issue of metal loss. A relatively effective way to annul the effect of the loss is via the use of the gain medium [3–5], such as GaAs/AlGaAs with a quantum well [6], or high index InGaAsP with optical pumping [7]. The incorporation of a gain medium in plasmonic devices is capable of achieving lossless gain-assisted SPP propagation [8], increasing the resolution of negative-refractive-index near-field lenses [9] and producing a large variation of the group velocity of nanoscale waveguides [10]. Meanwhile, the demonstration of 'plasmon laser' or 'spasers' has boosted the interest of new systems combining gain and plasmonics, like the metal-coated nanopillars [11], gold nanospheres [12] and metal hole arrays [13]. While the inherently high Joule losses are generally considered as harmful in plasmonic systems, in some cases they can play a positive role, e.g. for purposes of demonstration of an entangled steady state of two quantum qubits [14], the achievement of the plasmonic photothermal therapy with gold nanoparticles [15]

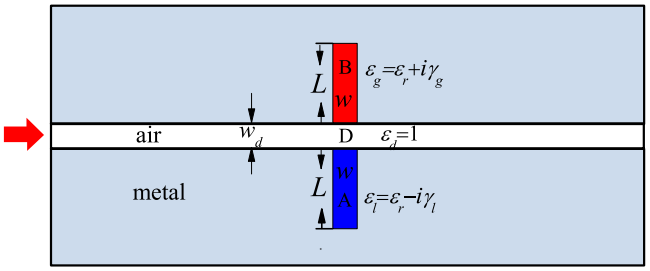

Figure 1. The scheme of the MDM SPP waveguide side-coupled two cavities. Cavity A and cavity B are respectively filled with lossy medium and gain medium.

and the realization of absorption induced transparency in the combined metal hole array plus dye system [16].

In recent years, much attention has been paid to the general combination of gain and loss, apart from the sole gain compensation and loss utilization. For example, the popular parity-time (PT) symmetric coupled pair of waveguides, one with gain and the other with loss in a symmetric amount, where the peculiar features of the gain and loss such as 'nonreciprocality' [17] and 'singular eigenvalue behavior' [18], can bring some possible applications including the optical switch [19] and memories [20]. In this study, the system of an MDM SPP waveguide with side-coupled cavity is employed as a platform to explore the combined effect of gain and loss. The gain medium or loss medium has already been introduced into such a system to act as a tunable absorption switch or gain switch [21, 22], where the effect of the single side-coupled lossy or gain cavity is concerned. Here, we respectively fill the gain medium and lossy medium into two equi-length side-coupled cavities. The issue that concerns us is exploring the competitive mechanism between the two cavities and the combined effect of the gain and loss on the system response. Some unexpected plasmonic responses are obtained, such as the occurrence of PIT [23, 24]-like transmission peaks for the case of balanced gain and loss, as well as the dissipative system response for the case with larger gain, and accumulative one for the case with larger loss, at around the resonant frequency of the two cavities.

2. Theoretical model and method

We consider an MDM SPP waveguide composite system consisting of two side-coupled rectangular cavities, as shown in figure 1. The waveguide backbone width is w_d, the lengths and widths of the two cavities are L and w. The metallic medium surrounding the waveguide backbone and the two cavities has the permittivity $\varepsilon_m=\varepsilon_\infty-\dfrac{\omega_p^2}{\omega(\omega+\mathrm{i}\gamma_m)}$ and the gap dielectric medium in the backbone is the air with $\varepsilon_d = 1$. The two cavities are filled with the semiconductor medium InGaAsP [22]; without pumping, the medium is lossy. With the increase of pump power, such a medium exhibits gain. We set the permittivity of the lossy InGaAsP in cavity A as $\varepsilon_l = \varepsilon_r - \mathrm{i}\gamma_l$ and the gain InGaAsP in cavity B as $\varepsilon_g = \varepsilon_r + \mathrm{i}\gamma_g$, both γ_l and γ_g are the positive real numbers.

Suppose the magnetic field at the input port is $H_0\mathrm{e}^{-\mathrm{i}\omega t}$, the fields in cavity A and cavity B are expressed as $H_A=A\mathrm{e}^{\mathrm{i}\phi_A}\mathrm{e}^{-\mathrm{i}\omega t}$ and $H_B=B\mathrm{e}^{\mathrm{i}\phi_B}\mathrm{e}^{-\mathrm{i}\omega t}$. A and B represent the amplitudes of two fields. ϕ_A and ϕ_B are the phases relative to the initial phase of the incident field. Based on the continuity condition of fields at the interfaces between the waveguide backbone and cavity A(B), we can obtain the following coupled-mode equations [25]

$$-\mathrm{i}G_l(\omega)+1]A\mathrm{e}^{\mathrm{i}\phi_A}-\kappa B\mathrm{e}^{\mathrm{i}\phi_B}=H_0, \tag{1a}$$

$$-\kappa A\mathrm{e}^{\mathrm{i}\phi_A}-[\mathrm{i}G_g(\omega)+1]B\mathrm{e}^{\mathrm{i}\phi_B}=H_0, \tag{1b}$$

where $\kappa = 1$ is the coupling coefficient between the two cavities, which means the direct interference effect of the two cavities. $\dfrac{1}{\mathrm{i}G_l(\omega)+1}$ and $\dfrac{1}{\mathrm{i}G_g(\omega)+1}$ respectively reflect the coupling of cavity A and cavity B with the waveguide backbone. G_l and G_g are the response functions of cavity A and cavity B with $G_l(\omega)=2Z_d/Z_l\cot(k_{spp}^l L_e)$ and $G_g(\omega)=2Z_d/Z_g\cot(k_{spp}^g L_e)$, respectively, where $L_e \approx L+w_d$ is the effective length of the cavity in our theoretical calculation. Z_η ($\eta = d, l, g$) are the impendences of SPP waveguide backbone D, the lossy cavity A and the gain cavity B [26],

$$Z_\eta=\frac{2k_{spp}^\eta}{\omega\varepsilon_\eta\sqrt{(k_{spp}^\eta)^2-\varepsilon_\eta k_0^2}}\tanh\left(\frac{\sqrt{(k_{spp}^\eta)^2-\varepsilon_\eta k_0^2}\,w_\eta}{2}\right), \tag{2}$$

and k_{spp}^η is the wave vector of SPP propagating in the waveguide. Here, we focus on the sub-wavelength MDM waveguide which only supports the symmetric TM_0 mode. The wave vector k_{spp}^η satisfies the dispersion relation [27]

$$\tanh\left(\frac{\sqrt{(k_{spp}^\eta)^2-\varepsilon_\eta k_0^2}\,w_\eta}{2}\right)=-\left(\frac{\varepsilon_\eta\sqrt{(k_{spp}^\eta)^2-\varepsilon_m k_0^2}}{\varepsilon_m\sqrt{(k_{spp}^\eta)^2-\varepsilon_\eta k_0^2}}\right). \tag{3}$$

The response functions are mainly dependent on the material parameters and the sizes of the cavities. This suggests the couplings between the two cavities and the backbone are determined by the material parameters and the sizes of the cavities. Note here that the incorporation of the gain and loss media in the two cavities makes the couplings become the complex numbers, thus the gain and loss parameters influence both the intensity and the phase of the fields localized in the two cavities. The corresponding solutions of equations (1a) and (1b) are

$$A\mathrm{e}^{\mathrm{i}\phi_A}=-\frac{G_g(\omega)H_0}{\mathrm{i}^*\,G_l(\omega)G_g(\omega)+G_l(\omega)+G_g(\omega)}, \tag{4a}$$

$$B\mathrm{e}^{\mathrm{i}\phi_B}=-\frac{G_l(\omega)H_0}{\mathrm{i}^*\,G_l(\omega)G_g(\omega)+G_l(\omega)+G_g(\omega)}. \tag{4b}$$

Evidently, the ratio of the field amplitudes of cavity B and cavity A is equal to the module ratio of the response functions of cavity A and cavity B,

$$B/A=|G_l(\omega)|/|G_g(\omega)|, \tag{5}$$

and the phase difference $\delta\phi = \phi_B - \phi_A$ between two cavities fields is

$$\mathrm{e}^{\mathrm{i}\delta\phi}=\frac{G_l(\omega)}{|G_l(\omega)|}\frac{G_g(\omega)^*}{|G_g(\omega)|}=\mathrm{e}^{\mathrm{i}(\phi_l-\phi_g)}, \tag{6}$$

where $\phi_l = \arg(G_l(\omega))$ and $\phi_g = \arg(G_g(\omega))$. It is found that $\delta\phi$ is equal to the argument difference of the response functions of two cavities.

The reflection coefficient r and the transmission coefficient t of the structure are obtained as [25, 26]

$$r = -\frac{G_g(\omega) + G_l(\omega)}{\mathrm{i}^* G_l(\omega)G_g(\omega) + G_l(\omega) + G_g(\omega)}, \tag{7}$$

$$t = -\frac{\mathrm{i}^* G_l(\omega)G_g(\omega)}{\mathrm{i}^* G_l(\omega)G_g(\omega) + G_l(\omega) + G_g(\omega)}, \tag{8}$$

furthermore, r and t can be rewritten as

$$r = r_g + r_l = r_l\left(1 + \left|\frac{G_l(\omega)}{G_g(\omega)}\right| \mathrm{e}^{\mathrm{i}\delta\phi}\right), \tag{9}$$

$$t = 1 - r_l\left(1 + \left|\frac{G_l(\omega)}{G_g(\omega)}\right| \mathrm{e}^{\mathrm{i}\delta\phi}\right), \tag{10}$$

with

$$r_{l(g)} = -\frac{G_{g(l)}(\omega)}{\mathrm{i}^* G_l(\omega)G_g(\omega) + G_l(\omega) + G_g(\omega)}. \tag{11}$$

$r_{l(g)}$ is interpreted as the reflection coefficient of cavity A(B) when considering the coupling effect between the two cavities. Thus the field amplitudes of the two cavities are given by $A = |r_l|H_0$ and $B = |r_g|H_0$. Note that $r_{l(g)}$ for our structure is distinguished from that for the waveguide system with single side-coupled cavity A or B, where the reflection coefficient is $-\frac{1}{\mathrm{i}G_{l(g)}(\omega) + 1}$ [25]. We find that the reflection coefficient r is the sum of r_g and r_l, which means the plasmonic response of the system is directly attributed to the interference of the two fields of the cavities.

From equations (9) and (10), the reflectance and the transmittance of this structure are given as

$$R = \frac{\frac{|G_l|}{|G_g|} + \frac{|G_g|}{|G_l|} + 2\cos(\delta\phi)}{\frac{|G_l|}{|G_g|} + \frac{|G_g|}{|G_l|} + 2\cos(\delta\phi) + |G_l||G_g| - 2(|G_l|\sin(\phi_g) + |G_g|\sin(\phi_l))}, \tag{12}$$

$$T = \frac{|G_g||G_l|}{\frac{|G_l|}{|G_g|} + \frac{|G_g|}{|G_l|} + 2\cos(\delta\phi) + |G_l||G_g| - 2(|G_l|\sin(\phi_g) + |G_g|\sin(\phi_l))}. \tag{13}$$

So the reflectance and the transmittance that have to do with the fields of the input and output waveguide ports are determined by both the phases and modulus of the response functions of two cavities.

3. Discussion

In this part, we first consider that the metal is loss-free ($\gamma_m = 0$). Two typical cases are discussed in detail. The two equi-length cavities are respectively filled with the same gain and loss and the two cavities with the different gain and loss. Obviously, the former corresponds to the balanced case of gain and loss and the latter belongs to the unbalanced case. Next we investigate the unbalanced case when the metal loss is included.

3.1. Balanced case

When the gain and loss is balanced ($\gamma = \gamma_g = \gamma_l$), the effective complex refractive index of the two cavities satisfy $n_A = n_B^*$, so the SPP propagating through the two cavities obeys the PT symmetric condition [28, 29]. Under this situation, $|G_g(\omega)| = |G_l(\omega)|$ and $\phi_g(\omega) = -\phi_l(\omega)$, the fields of the two cavities are always equi-amplitude and out of phase. From the equations (12) and (13), the sum of transmittance and reflectance is always equal to 1. Therefore, the remarkable feature of our system response, comparing with that of the system side-coupled two cavities without gain and loss, is the existence of the phase difference between the two cavities induced by the gain and loss.

Specifically, in our calculation, the metal medium in the waveguide is supposed to be silver with the parameters $\varepsilon_\infty = 3.7$, $\omega_p = 1.38 \times 10^{16}$ Hz [30], the sizes of the waveguide and cavities are $L = 100$ nm, $w_d = w = 30$ nm and the amplitude of the initial incident field is set as $H_0 = 1$. Because the dielectric dispersion doesn't break the competitive mechanism for the gain and lossy cavities, its dispersive effect on the system response is minor. For simplicity, we ignore the dispersion of InGaAsP in frequencies by setting the real part of permittivity as a constant $\varepsilon_r = 11.38$ [22, 31] and the gain and loss parameters as $\gamma_g = \gamma_l = 0.165$. The reflectance R, the transmittance T, the field amplitudes $A(B)$ and the phase difference $|\delta\phi|$ as a function of frequency are plotted in figure 2(a). We can see the two fields are always equi-amplitude ($A = B$) and have a phase difference that attains a maximum value π at around the frequency of $\omega_0 = 317.6$ THz, where a PIT-like transmission peak appears. ω_0 is the resonant frequency of the two cavities and is obtained from the Fabry–Perot resonant condition $\mathrm{Re}\,(k_{spp}^{l(g)})L_e = \pi/2 + n\pi (n = 0, 1, \cdots)$. For the small parameter γ, the resonant frequency has a weak dependence on γ due to $\gamma \ll 11.38$. ω_0 thus can approximately be taken as a constant, since the variation of ω_0 is very small. The corresponding simulated field distribution at the frequency ω_0, where $A = B$ and $|\delta\phi| = \pi$, is depicted in figure 3(a). A physical origin for this plasmonic response, derived from equation (9), is attributed to the completely destructive interference of equal-amplitude fields at around the resonant frequency; a full transparency is thus realized ($T = 1$). While shifting from this frequency, $|\delta\phi| < \pi$, the interference cancellation of the two cavities is not complete. For comparison, the previous work of PIT realization in reference [23], where two detuned side-coupled Fabry–Perot resonators can be simplified as two unequal-length side-coupled cavities, is shown in figure 2(b). It can be seen that the phase difference, which is hopping with the variation of the frequency, only takes two values: 0 and π. At the range of frequencies $|\delta\phi| = \pi$, $A = B$ only falls at one frequency between the resonant frequencies of the two cavities, thus a transmission peak is achieved in the background of the stop band. Therefore, the generation mechanism of the PIT-like feature in our structure is different from that of previous PIT work.

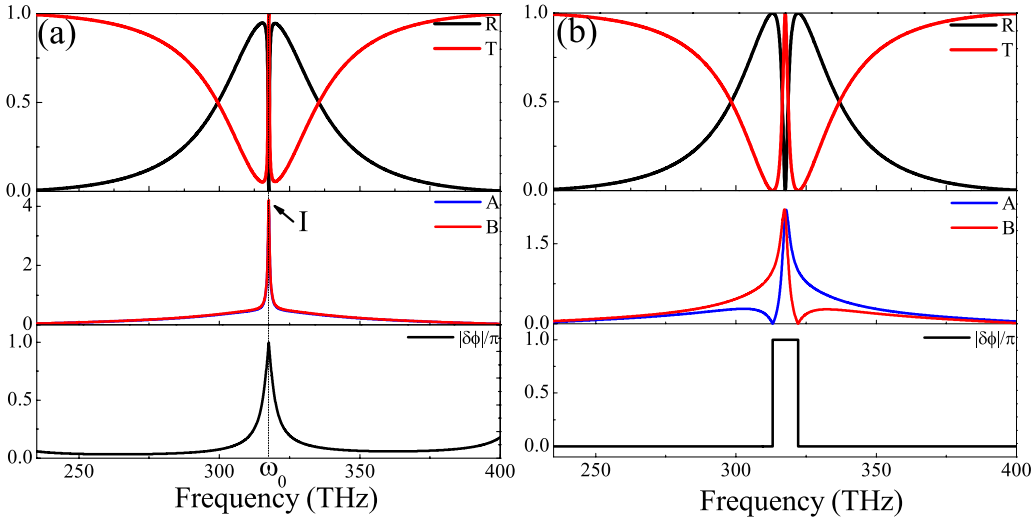

Figure 2. The reflectance R, the transmittance T, the phase difference $|\delta\phi|$ and the two field amplitudes $A(B)$ versus the frequency. (a) $\gamma_g = \gamma_l = 0.165$, $L = 100$ nm; (b) $\gamma_g = \gamma_l = 0$, $L_A = 104$ nm, $L_B = 98$ nm. $w_d = w = 30$ nm and $H_0 = 1$ for both two cases.

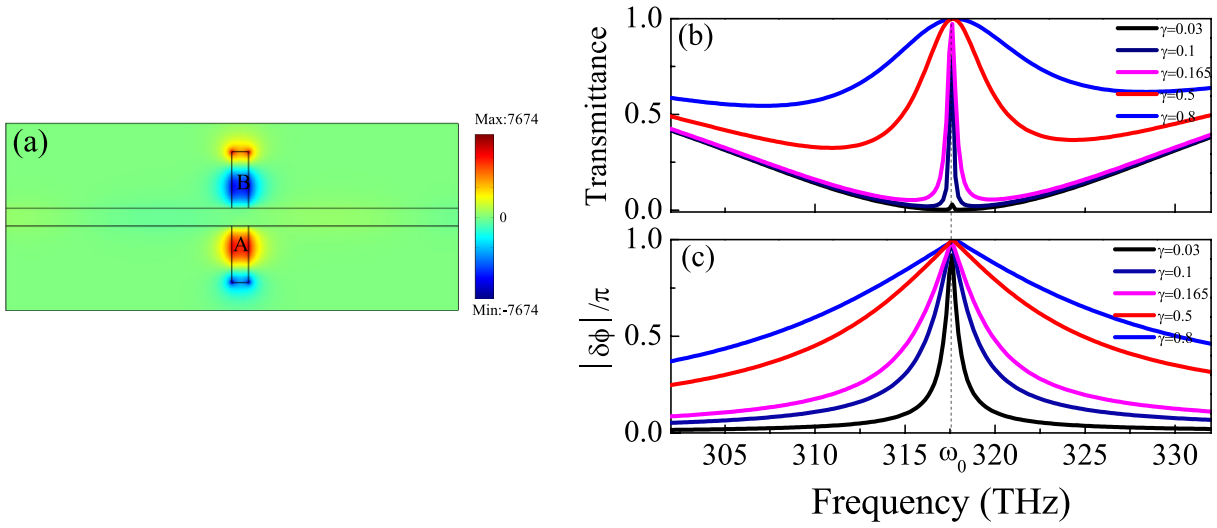

Figure 3. (a) The magnetic field distribution of the structure at the frequency 317.6 THz (marked with I in figure 2(a)) for $\gamma_g = 0.165$, $\gamma_l = 0.165$, where $|\delta\phi| = \pi$ and $A = B$; The transmittance $T(b)$ and the phase difference $|\delta\phi|(c)$ as the function of frequency for different γ. Other geometrical parameters are the same: $L = 100$ nm, $w_d = w = 30$ nm.

To investigate the influence on the plasmonic response made by the parameter γ, the transmittance and the phase difference $|\delta\phi|$ for different γ are plotted in figure 3(b). For $\gamma = 0$, it is shown that the two cavities are always in phase ($|\delta\phi| = 0$): no transmission peak is observed. For $\gamma > 0$, $|\delta\phi| \neq 0$, the disharmony of the two cavity responses starts to emerge. As γ increases from zero, the maximum of $|\delta\phi|$ becomes larger and the transmission peak becomes higher. It also shows that the increase of γ results in the larger line-width of the phase difference; accordingly, the transmission peak becomes blunter. When γ reaches 0.165, the maximum of $|\delta\phi|$ attains π; the largest transmission peak ($T = 1$) is obtained. When γ increases further, the peak no longer becomes higher but it trends to the pass-band. In addition, with increasing γ, the frequency of the transmission peak and the maximal phase difference remains close to ω_0 without evident shift. Thus the variation of γ makes little difference to the frequency of the transmission peak but has a large impact on the line shape of the transmission spectrum.

3.2. Unbalanced case

In this case, the system response is associated with the interference of the two fields which are neither equal-amplitude nor in-phase ($A/B \neq 1$ and $|\delta\phi| \neq 0$). For simplicity, we focus on the following two unbalanced cases without considering the metal loss: (1) $\gamma_g > \gamma_l$; (2) $\gamma_g < \gamma_l$. The transmittance and reflectance spectra for $\gamma_g = 0.15$, $\gamma_l = 0.06$ and $\gamma_g = 0.06$, $\gamma_l = 0.15$ are depicted in the figures 4(a) and (b), respectively. Like the balanced case, the peak or dip of reflection and transmission, as well as the maximal phase difference, also appear at around the resonant frequency of two cavities. Besides, in the

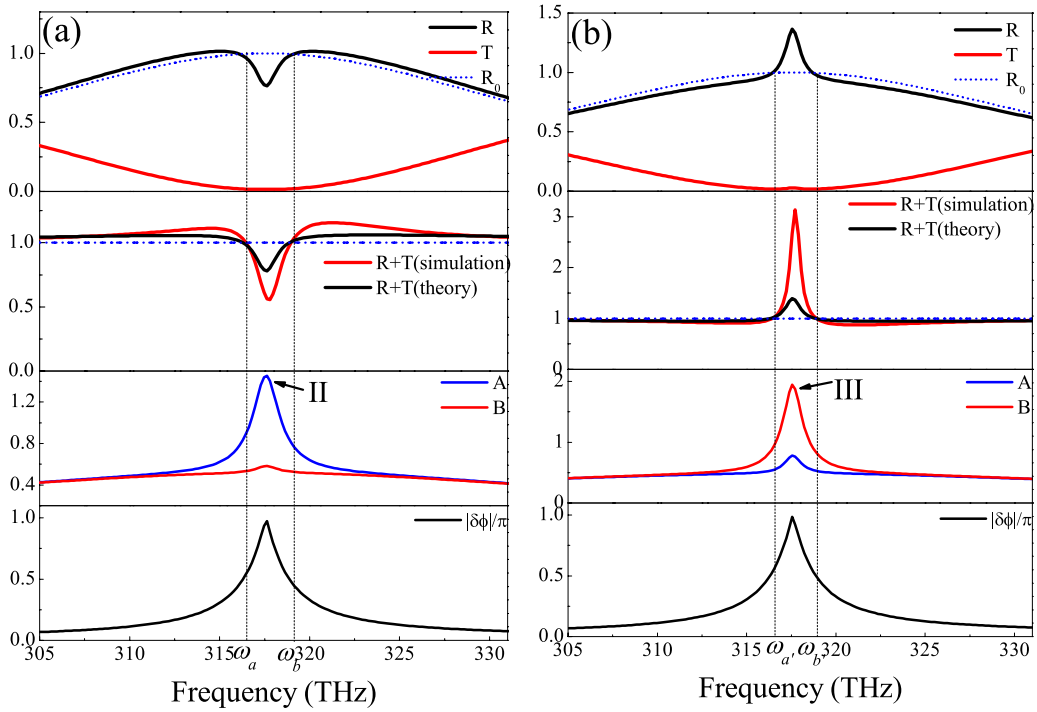

Figure 4. The reflectance R, the transmittance T, the phase differences $|\delta\phi|$ and the amplitudes $A(B)$ of two fields versus the frequency. (a) $\gamma_g = 0.15$, $\gamma_l = 0.06$; (b) $\gamma_g = 0.06$, $\gamma_l = 0.15$; R_0 represents the reflectance for $\gamma_g = \gamma_l = 0$. Other parameters are the same: $L = 100$ nm, $w_d = w = 30$ nm, $H_0 = 1$.

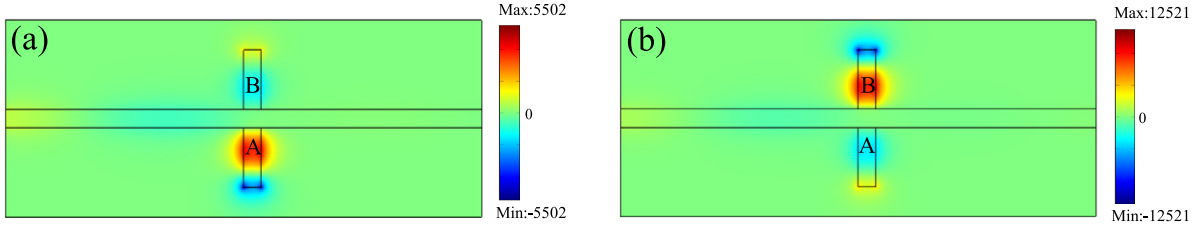

Figure 5. The magnetic field distributions of the structure at the frequency 317.6 THz (marked with II,III in figure 4), where $|\delta\phi| = \pi$. $A > B$ for (a) $\gamma_g = 0.15$, $\gamma_l = 0.06$; $A < B$ for (b) $\gamma_g = 0.06$, $\gamma_l = 0.15$; Other geometrical parameters are the same: $L = 100$ nm, $w_d = w = 30$ nm.

figure 4(a), the reflection spectrum appears as a dip together with no transmission peak in the transmission spectrum for $\gamma_g = 0.15$, $\gamma_l = 0.06$. While for $\gamma_g = 0.06$, $\gamma_l = 0.15$, we can see the transmission peak is still not obvious, though the reflection curve appears as a peak in figure 4(b) and this sharp reflection peak is larger than the reflection background.

Next, we give a qualitative analysis of the variations of the system response for the above two cases: for $\gamma_g = 0.15$, $\gamma_l = 0.06$, as shown in figure 4(a), in the ranges of frequencies $\omega<\omega_a$ and $\omega>\omega_b$ (ω_a and ω_b are the critical frequencies corresponding to $R + T = 1$), $|\delta\phi|$ is relatively small. Two cavity responses are not sensitive to the gain and loss and the reflectance spectrum has a reflection background that is similar to R_0 which is the reflectance of the waveguide side-coupled to two cavities without gain and loss. In these ranges of frequencies, the system response is accumulative ($R+T > 1$). This is because the cavity with the larger gain makes the dominant effect on the response. In the range of frequencies $\omega \in (\omega_a, \omega_b)$, the system response turns into dissipative one ($R+T < 1$). The reason for the transition of the system response is that—based on equation (5) involving the field amplitude, the larger gain or loss parameter corresponding to the larger module of the response function—the weaker field is localized in the cavity at around the resonant frequency. Thus we can see that there is a much stronger field localized in the lossy cavity than that in the gain cavity in figure 4(a); the simulated magnetic field distribution at 317.6 THz where $A > B$ is shown in figure 5(a). The dissipation effect of the lossy cavity enhanced by the stronger field overwhelms the amplification effect of the cavity with larger gain, thus the lossy cavity makes a main contribution to the system response. By contrast, for $\gamma_g = 0.06$, $\gamma_l = 0.15$, at the ranges of $\omega<\omega_{a'}$ and $\omega>\omega_{b'}$ ($\omega_{a'}$ and $\omega_{b'}$ are the critical frequencies corresponding to $R+T = 1$), the reflection curve also has a reflection background similar to the R_0. The system response is dissipative ($R+T < 1$) because the cavity with the larger loss makes the dominant effect on the response. At the range of $\omega\in(\omega_{a'}, \omega_{b'})$, the system response becomes accumulative ($R+T > 1$). This is because $A < B$, as shown in figures 4(b) and 5(b): the strongly localized field enhances the amplification effect of the gain cavity, so the system supports the occurrence of the reflection peak larger than the reflection background.

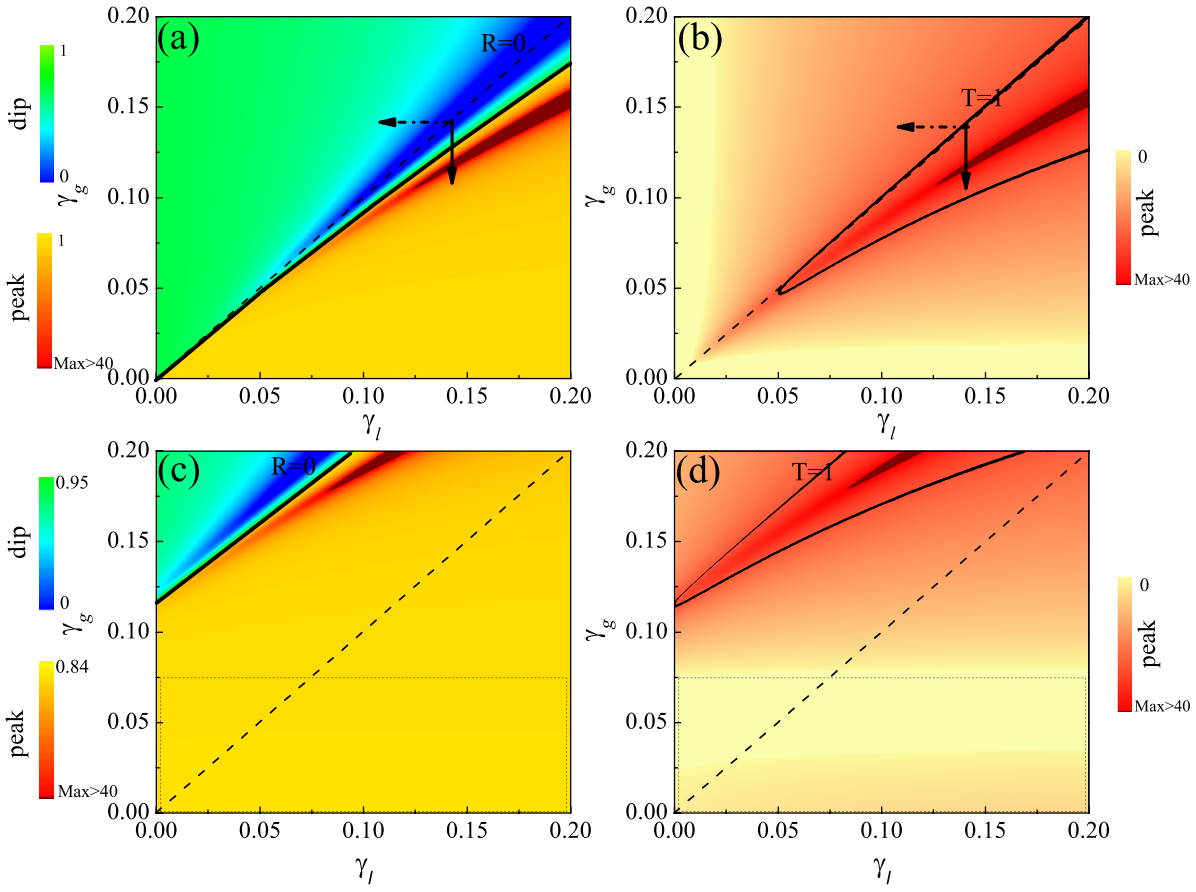

Figure 6. The reflection dip or peak (*a*) and the transmission peak (*b*) as the functions of γ_g and γ_l for $\gamma_m = 0$. The reflection dip or peak (*c*) and the transmission peak (*d*) as the functions of γ_g and γ_l for $\gamma_m = 2.73 \times 10^{13}$ Hz. Other geometrical parameters are the same: $L = 100$ nm, $w_d = w = 30$ nm.

From figures 3 and 4 it can be concluded that the frequency positions of the peak and dip in the reflection and transmission spectra have a weak dependence on the γ_g and γ_l parameters, though the values of the peak and dip are significantly affected by the γ_g and γ_l parameters. In detail, the reflection dip $\left(\frac{\partial^2 R}{\partial \omega^2}\Big|_{\omega\approx\omega_0} > 0\right)$ or peak $\left(\frac{\partial^2 R}{\partial \omega^2}\Big|_{\omega\approx\omega_0} < 0\right)$ and the transmission peak $\left(\frac{\partial^2 T}{\partial \omega^2}\Big|_{\omega\approx\omega_0} < 0\right)$ as functions of the γ_g and γ_l are depicted in figures 6(*a*) and 6(*b*), respectively. For $\gamma = \gamma_g = \gamma_l$, corresponding to the balanced case that has been discussed above, the reflection dip becomes deeper and the transmission peak becomes higher as increasing γ until they become the deepest dip ($R = 0$) and the PIT-like peak ($T = 1$), respectively. For $\gamma_g > \gamma_l$, the lossy cavity makes the dominant effect on the system response, the sum of reflectance and transmittance is less than 1, the system response is dissipative at around the resonant frequency. When γ_g is fixed, as γ_l decreases, starting from the diagonal line (the virtual arrow in figure 6(*a*)), the reflection dip becomes shallower due to the incomplete destructive interference between the two fields with the larger difference in amplitudes. The value of the transmission peak is less than 1 and becomes smaller as shown in figure 6(*b*). For $\gamma_g < \gamma_l$, the gain cavity makes the dominant effect on the system response, the sum of reflectance and transmittance is larger than 1, the system response is accumulative. When keeping γ_l fixed, as γ_g decreases along the direction denoted by the solid arrow in the graph, the reflection dip becomes shallower and the transmission peak becomes higher. With continued decreasing of γ_g, the system continues to accumulate, the reflection curve thus exists as a transition from the dip to the peak, which is larger than the reflection background. When the system reaches the largest accumulative state, the reflection and transmission peaks increase to become the largest peaks. By further decreasing γ_g, the amplification effect of the gain cavity is suppressed by the decrease of γ_g and the transmission peak and reflection peak start to become smaller as observed in figures 6(*a*) and (*b*), respectively.

In the following, we consider the influence of the metal loss on the system response ($\gamma_m > 0$). The metal loss yields two main effects on the system response. Obviously, the first effect is the dissipation of the system energy, so the reflectance and the transmittance of the structure are reduced accordingly as a whole. The second effect mainly takes place at around the resonant frequency of the two cavities, where the dramatic effect of the gain cavity and lossy cavity on the system response is exhibited. The reflection peak or dip and the transmission peak

as the functions of γ_g and γ_l for $\gamma_m = 2.73 \times 10^{13}$ Hz thus are plotted in figures 6(*c*) and (*d*), respectively. We can see the region of the deepest reflection dip, the reflection transition line and the transmission isoline with the value 1 have some shift along the positive direction of the γ_g axis and the negative direction of the γ_l axis compared to the case of absence of metal loss, namely the region where the gain cavity produces the dominant effect is extended to some regions of $\gamma_g > \gamma_l$. This can be interpreted as: the metal loss increases the effective loss of the lossy cavity but reduces the effective gain of the gain cavity. The larger effective loss in the lossy cavity promotes the stronger field that is localized in the gain cavity. Therefore, the metal loss facilitates the gain cavity to have a major effect on the system response. Moreover, in the region marked with the virtual rectangle, the sum of the reflectance and transmission is less than 1. This suggests that although the gain cavity has the main effect on the system in this region, with the amplification effect hampered by the metal loss, so the sum of the reflectance and the transmittance is possibly less than 1. In addition, the system still sustains the PIT-like response which does not occur at $\gamma_g = \gamma_l$ but $\gamma_g > \gamma_l$ when the metal loss is considered. The extra gain is used for compensating the metal loss.

4. Conclusion

Using the MDM SPP waveguide with two side-coupled cavities filled with one lossy medium and one gain medium as a platform, the combined effect of gain and loss on the system response has been theoretically investigated using Green's function method. The results show that both the amplitude and phase of the fields localized in two cavities are influenced by the gain and loss parameters. When two equi-length cavities are filled with the balanced gain and loss, a PIT-like transmission peak is achieved owing to the destructive interference of the phase-opposite and equi-amplitude fields of the two cavities. For the unbalanced case, some unexpected plasmonic responses were obtained. When the gain is more than the loss, the sum of the reflectance and the transmission becomes less than 1 at around the resonant frequency of the two cavities, corresponding to a dissipative system response. This is because the dissipation effect of the lossy cavity enhanced by the stronger localized field can beat the amplification effect of the cavity with a larger gain, thus the lossy cavity has a dominant effect on the system response. The situation changes, however, when the gain is less than the loss. Our investigation also suggests that the metal loss dissipates the system energy but that it is favorite for the major role of the gain cavity. This mechanism may be useful for the applications of the optical amplifier and the switch in an SPP-based integrated structure.

Acknowledgments

We acknowledge financial support from the National Natural Science Foundation of China grant no. 11174222 and the National Basic Research Program (973) of China grant no. 2011CB922203.

References

[1] Bozhevolnyi S I, Volkov V, Devaux E, Laluet J and Ebbesen T 2006 *Nature* **440** 508
[2] Gan Q, Gao Y, Wang Q, Zhu L and Bartoli F 2010 *Phys. Rev.* B **81** 085443
[3] Leon I D and Berini P 2008 *Phys. Rev.* B **78** 161401
[4] Maier S A 2006 *Opt. Commun.* **258** 295
[5] Handapangoda D, Rukhlenko I D and Premaratne M 2013 *J. Opt.* **15** 035006
[6] Li D B and Ning C Z 2009 *Phys. Rev.* B **80** 153304
[7] Saitoh T and Mukai T 1987 *IEEE J. Quantum Electron.* **QE-23** 1010
[8] Nezhad M, Tetz K and Fainman Y 2004 *Opt. Express* **12** 4072
[9] Ramakrishna S A and Pendry J B 2003 *Phys. Rev.* B **67** 201101
[10] Govyadinov A A and Podolskiy V A 2006 *Phys. Rev. Lett.* **97** 223902
[11] Hill M T *et al* 2007 *Nature Photon.* **1** 589
[12] Noginov M A, Zhu G, Belgrave A M, Bakker R, Shalaev V M, Narimanov E E, Stout S, Herz E, Suteewong T and Wiesner U 2009 *Nature* **460** 1110
[13] Beijnum F, Veldhoven P J, Geluk E J, Dood M J A, Hooft G W and Exter M P 2013 *Phys. Rev. Lett.* **110** 206802
[14] Lin Y, Gaebler J P, Reiter F, Tan T R, Bowler R, Sørensen A S, Leibfried D and Wineland D J 2013 *Nature* **504** 415
[15] Huang X H, Jain P K, El-Saye I H and El-Sayed M A 2008 *Lasers Med. Sci.* **23** 217
[16] Rodrigo S G, García-Vidal F J and Martín-Moreno L 2013 *Phys. Rev.* B **88** 155126
[17] Čtyroký J 2014 *Opt. Quantum Electron.* **46** 465
[18] Benisty H *et al* 2011 *Opt. Express* **19** 18004
[19] Lupu A, Benisty H and Degiron A 2013 *Opt. Express* **21** 21651
[20] Rüter C E, Makris K G, El-Ganainy R, Christodoulides D N, Segev M and Kip D 2010 *Nature Phys.* **6** 192
[21] Min C j and Veronis G 2009 *Opt. Express* **17** 10757
[22] Yu Z, Veronis G, Fan S and Brongersma M L 2008 *Appl. Phys. Lett.* **92** 041117
[23] Han Z H and Bozhevolnyi S I 2011 *Opt. Express* **19** 3251
[24] Lu H, Liu X M and Mao D 2013 *Phys. Rev.* A **85** 053803
[25] Tan W, Yang C Z, Liu H S, Wang Z G, Lin H Q and Chen H 2012 *Europhys. Lett.* **97** 24003
[26] Zhu Q G and Wang Z G 2013 *Europhys. Lett.* **103** 17004
[27] Lin C-I and Gaylord T K 2012 *Phys. Rev.* B **85** 085405
[28] Longhi S 2009 *Phys. Rev. Lett.* **103** 123601
[29] Mostafazadeh A 2013 *Phys. Rev.* A **87** 012103
[30] Han Z, Forsberg E and He S 2007 *IEEE Photon. Technol. Lett.* **19** 91
[31] Bi W G and Li A 1992 *J. Appl. Phys.* **71** 2826